Korean Chem. Eng. Res., 57(3), 368-371 (2019)
https://doi.org/10.9713/kcer.2019.57.3.368
PISSN 0304-128X, EISSN 2233-9558

First-Principles Study on Thermodynamic Stability of UO_2 with He Gas Incorporation via Alpha-Decay

Choa Kwon*, Kwanpyung Lee and Byungchan Han***,†**

**Department of Chemical and Biomolecular Engineering, Yonsei University, 50, Yonsei-ro, Seodaemun-gu, Seoul, 03722, Korea*
***Department of Chemical and Biomolecular Engineering, Yonsei University, 50, Yonsei-ro, Seodaemun-gu, Seoul, 03722, Korea*
****Department of Chemical and Biomolecular Engineering, Yonsei University, 50, Yonsei-ro, Seodaemun-gu, Seoul, 03722, Korea*
(Received 25 February 2019; accepted 2 April 2019)

Abstract – Using first principles calculations we investigated the thermomechanical stability of spent nuclear fuels (SNF), especially how mechanical properties of UO_2, such as, bulk, shear and Young's moduli and Poisson's ratio vary through alpha-decay of U into Th with generation of He gas. Our results indicate that substitution of U by Th through alpha decay ($U_{1-x}Th_xO_2$) does not significantly affect the stability of the grain in a fuel matrix. In addition, we studied the transport properties of He in and boundaries of the $U_{1-x}Th_xO_2$ grain. Helium preferentially resides at the grain boundaries through diffusion. Our study can contribute to substantial reduction of environmentally risk and enhancement of our sustainability by safe control of radioactive materials.

Key words: First-principles, Uranium dioxide, Alpha decay, Thermodynamic stability, Helium gas

1. Introduction

Uranium dioxide (UO_2) has been a key nuclear fuel, yet in spite of many benefits of nuclear energy, the safe and economic, disposal of radioactive waste is global concern [1,2]. Especially, highly radioactive spent nuclear fuels (SNFs) are the central materials for the handling [3]. Recently, reducing the radioactivity and volume through pyroprocessing technology was studied, but still long-term storage or permanent disposal of SNFs in deep earth is the major way.

In the disposed SNFs, a large quantity of helium (He) gas can be generated and coalesced into bubbles in the fuel matrix, which may lead to swelling of the materials [4]. To improve the safety level, there have been many experimental or theoretical studies on the behavior of He in the fuel matrix [5-7]. For example, the stability of He was evaluated by calculating its incorporation energy in the grain [8,9]. It was reported that He thermodynamically does not stay in the interstitial sites of bulk UO_2 since the incorporation energy is very high (0.72~0.89 eV per He atom). In addition, activation energies of He for diffusion in bulk UO_2 were calculated as 2.2~4.15 eV [5,8] and measured as 1.87~2.23 eV [9,10] meaning the process is, in fact, difficult.

Since an alpha decay of U into Th is of importance for the production of He [11], a pure UO_2 may not be a relevant model system for studying SNF stability. In this study, we calculated moduli and Poisson's ratio of $U_{1-x}Th_x O_2$ to identify variation of the mechanical strength as a function of Th composition. Using first-principles calculations the incorporation energy and diffusion energy barrier of He in the $U_{1-x}Th_xO_2$ at x = 0.0, 0.13 and 0.25 were predicted. Since UO_2 pellet is a poly-crystalline [12], we set up a Σ3(111) tilt grain boundary model, which is one of common grain boundaries [13,14] to investigate stability of SNF.

2. Computational Details

All calculations in this study were carried out as density functional theory calculations as implemented in Vienna ab initio simulation package (VASP) [15]. The generalized gradient approximation (GGA) with Perdew-Burke-Ernzerhof (PBE) [16,17] was used for exchange correlation functional, and the projected augmented wave (PAW) potentials [18] were used to substitute core electrons of U, Th, O and He. Convergence criteria for ionic relaxation for all calculations were energy difference less than 10^{-5} eV compared to the right before step. For bulk properties, such as incorporation energies and mechanical properties, the k-points sampling was conducted on a 4 × 4 × 4, while for grain boundaries 5×5×3 mesh was used. We performed calculations including the effective Hubbard correction in the GGA+U approximation to correct the localized f electrons of uranium, using U_{eff} = 3.96 eV [14,19] with U-ramping scheme [20,21] to optimize ground state of UO_2.

3. Results and Discussion

3-1. Stability of fuels in a grain of $U_{1-x}Th_xO_2$

As both UO_2 and ThO_2 have cubic fluorite structures (a = 5.47 for

† To whom correspondence should be addressed.
E-mail: bchan@yonsei.ac.kr
‡This article is dedicated to Prof. Yong-Gun Shul on the occasion of his retirement from Yonsei University.

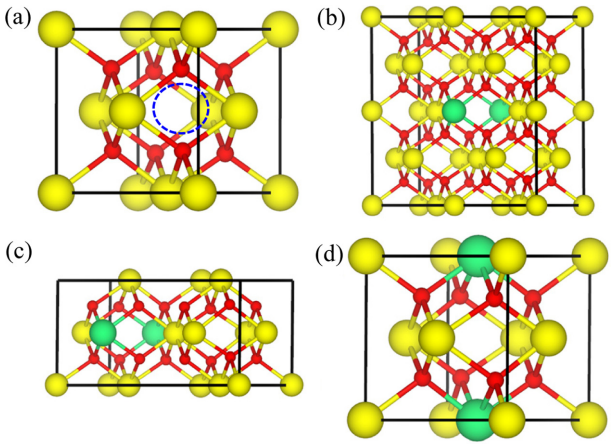

Fig. 1. Model systems of (a) UO_2 (b) $U_{0.94}Th_{0.06}O_2$ (c) $U_{0.87}Th_{0.13}O_2$ and (d) $U_{0.75}Th_{0.25}O_2$ to calculate incorporation energies. Yellow, green and red atoms indicate U, Th and O, respectively. The blue circle in (a) indicates OIS.

UO_2, a = 5.60 for ThO_2) [22], 1 × 1 × 1 unit cells of $U_{1-x}Th_xO_2$ were employed to model $U_{1-x}Th_xO_2$ matrix. An octahedral interstitial site (OIS) [23,24] was considered for He atom in the matrix as shown in Fig. 1. Supercells of 2 × 1 × 1 and 2 × 2 × 1 of UO_2 were used, and in each supercell a U atom was replaced by Th atom to describe $U_{0.87}Th_{0.13}O_2$ and $U_{0.94}Th_{0.06}O_2$, respectively, via alpha decay.

The incorporation energy was defined as Eq. (1) ,

$$E_{inc} = E_{bulk+He} - (E_{bulk} + E_{He}) \quad (1)$$

E_{inc} represents incorporation energy, $E_{bulk+He}$ is total energy of the model $U_{1-x}Th_xO_2$ with He at the OIS, E_{bulk} is the total energy of the $U_{1-x}Th_xO_2$ without He and E_{He} is the energy of non-interacting He atom.

Incorporation energies of $U_xTh_{1-x}O_2$ were 0.89, 0.85, 0.91 and 0.90 eV at x = 0.0, 0.06, 0.13 and 0.25 as shown in Fig. 2(a), and activation barriers of He in UO_2 and $U_{0.03}Th_{0.97}O_2$ obtained by nudged elastic band (NEB) method [9,10] are illustrated in Fig. 2(b). Since E_{inc} in $U_{1-x}Th_xO_2$ are positive He is thermodynamically unstable in $U_{1-x}Th_xO_2$. It implies that He prefers diffusing out of the grain and into grain boundary or more open space. Diffusion activation barriers of He between OIS in UO_2 and $U_{0.97}Th_{0.03}O_2$ were estimated as 2.39 eV and 2.40 eV, respectively, as shown in Fig. 2(b). These values are similar because bond strength Th-O are stronger than U-O. In the diffusion process in UO_2 the diffusing He only elongates U-O bond length from 2.39 to 2.52 Å, while Th-O bond length remains the same. This feature is the same in $U_{0.97}Th_{0.03}O_2$ even when He moves beside Th.

3-2. Mechanical strength of $U_xTh_{1-x}O_2$

For a cubic crystal, three independent elastic constants (C_{11}, C_{12}, and C_{44}) [25] are defined. C_{44} can be obtained from applying a monoclinic volume-conserving distortion matrix, Δ_{mono} to a relaxed unit cell [25].

$$\Delta_{mono} = \begin{pmatrix} 1 & \delta/2 & 0 \\ \delta/2 & 1 & 0 \\ 0 & 0 & 4/(4-\delta^2) \end{pmatrix}$$

where δ = -0.1, -0.05, 0.05 and 0.1. The energy increase per unit cell volume $E(\delta)$ is given by Eq. (2),

$$E(\delta) = C_{44}\delta^2 + O(\delta^3) \quad (2)$$

Tetragonal shear constant C′ [C′ = ((C11+C12)/2)] can be obtained from applying a tetragonal volume-conserving distortion matrix, Δ_{tetra} to a relaxed unit cell [25].

$$\Delta_{tetra} = \begin{pmatrix} 1+\delta & 0 & 0 \\ 0 & 1-\delta & 0 \\ 0 & 0 & 1/(1-\delta^2) \end{pmatrix}$$

where δ = -0.1, -0.05, 0.05 and 0.1. The energy increase per unit cell volume $E(\delta)$ is also related to the tetragonal shear constants as Eq. (3),

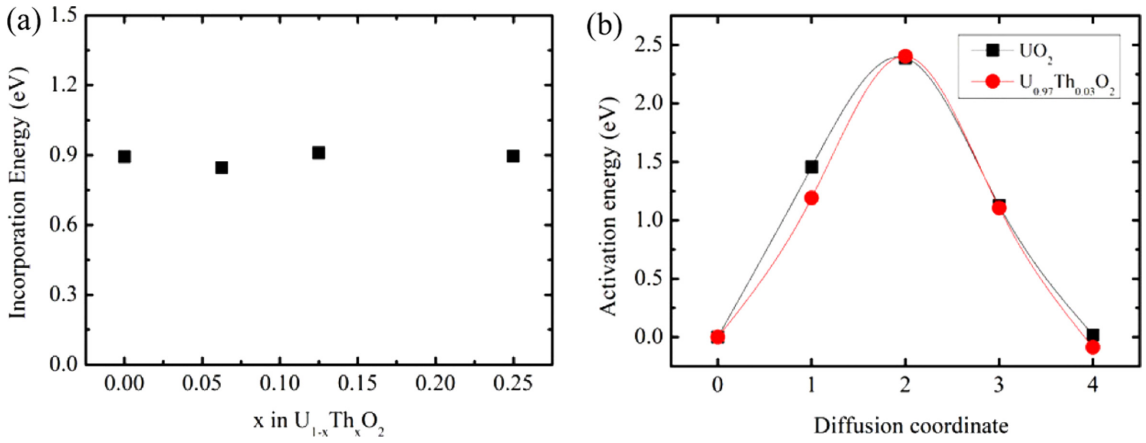

Fig. 2. (a) Incorporation energy of $U_{1-x}Th_xO_2$ at x = 0.89, 0.85, 0.91 and 0.90. (b) Energy variations of UO_2 and $U_{0.97}Th_{0.03}O_2$ when He atom diffuses from OIS to another nearest OIS.

$$E(\delta) = C'\delta^2 + O(\delta^3) \quad (3)$$

Bulk modulus, B, can be similarly obtained from a volume-changing matrix to a relaxed unit cell. Here, we used the volume changes of -10 %, -5 %, 5 % and 10 % to the relaxed unit cell volume, respectively. From the tetragonal shear constant and bulk modulus, C_{11} and C_{12} were obtained [$B = (C_{11} + 2C_{12})/3$].

From these elastic constants, we calculated shear moduli (G) and Poisson's ratio (ν). The G can be calculated by the Hershey-Kröner averaging method relation [25,26] by which poly-crystalline effect is considered as shown in Eq. (4).

$$8G^3 + \left(9B + 4C'\right)G^2 - 3C_{44}\left(B + 4C'\right)G - 6BC_{44}C' = 0 \quad (4)$$

Young's modulus (E) is obtained from the relation between bulk and shear moduli [25,27] as Eq. (5).

$$E = \frac{9BG}{3B + G} \quad (5)$$

Poisson's ratio ν is obtained from bulk and Young's moduli [25] as Eq.(6).

$$\nu = \frac{3B - E}{6B} \quad (6)$$

We calculated elastic constants to obtain moduli and Poisson's ratio with respect to x in $U_{1-x}Th_xO_2$, where x is 0, 0.25, 0.5, 0.75 and 1.0, which are represented in Table 1.

Our calculations for Poisson ratios for UO_2 (0.251) and ThO_2 (0.220) are slightly smaller than experimentally measured ones (0.291~0.302 [28] and 0.279 [29], respectively). It can be ascribed to the anharmonicity in the moduli of the materials. From the results, the mechanical strength of UO_2 does not significantly change when the substitutional defects of U ions to Th ions are generated.

3-3. Stability of He in the grain boundary

Σ3(111) tilt grain boundary is one of the most abundant coincident site lattice (CSL) boundaries [14]. This boundary consists of two (111) planes as shown in the Fig. 3. Grain boundary energy and surface energy are defined as Eq. (6-1) and (6-2).

$$E_{gb} = \frac{E_{tot}(gb) - N_{gb}E_{bulk}}{2A_{gb}} \quad (6\text{-}1)$$

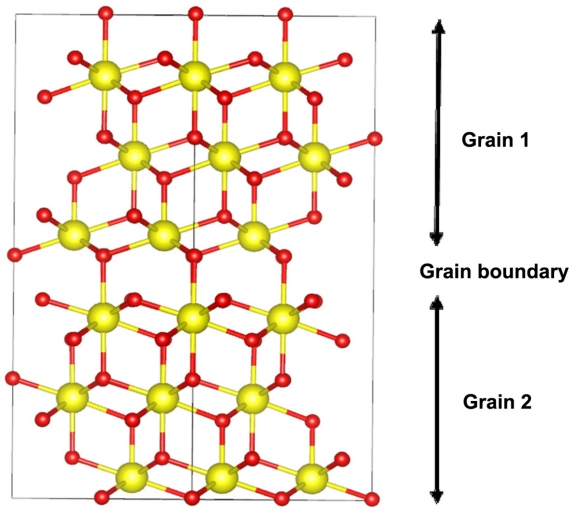

Fig. 3. Structure of Σ3 (111)/[110] tilt grain boundary and Position of a helium atom along the grains.

$$E_{surf} = \frac{E_{tot}(surf) - N_{surf}E_{bulk}}{2A_{surf}} \quad (6\text{-}2)$$

where E_{tot} (gb) and E_{tot} (surf) indicate total energy of grain boundary and surface of UO_2, respectively, and E_{bulk} does the energy of a pristine bulk UO_2 per formula unit. N_x and A_x represent number of UO_2 units in the system x and a cross-sectional area of the system x. If $E_{gb} - 2E_{surf} < 0$ two grains with grain boundaries are more stable than two non-interacting grains with terminated by (111) surfaces. As we calculated grain boundary energy E_{gb} = 0.057 eV/Å^2 and surface energy E_{surf} = 0.053 eV/Å^2 the Σ3(111) tilt grain boundary is more stable than two grains with terminated with (111) surfaces supporting experimental observation.

We calculated incorporation energies of a He atom for three different locations near the grain boundary shown in Fig. 3. The grain boundary incorporation energy of He was calculated as 0.85 eV, which is, in comparison with a pristine bulk, lower by 0.05 eV. It means He more easily resides at the more open grain boundary than inside bulk grain (the distance between two U atoms at the grain boundary increases from 3.17 Å to 3.30 Å. Therefore, we found that helium becomes more stable as helium migrates to the Σ3(111) tilt grain boundary.

Table 1. Shear modulus, Young's modulus

Compound	B	G	E	ν
UO_2	192.0	114.6	286.7	0.251
	192-240 [30]	80-105 [25]	-	0.30-0.34 [25]
	209-221 [31]	83 [31]	-	0.29-0.30 [28]
$U_{0.75}Th_{0.25}O_2$	190.1	138.6	334.6	0.206
$U_{0.50}Th_{0.50}O_2$	246.9	153.7	381.8	0.242
$U_{0.25}Th_{0.75}O_2$	193.9	121.4	301.3	0.241
ThO_2	189.1	129.7	316.7	0.220
	198 [22]	100 [32]	-	0.279 [29]

4. Conclusion

We performed first-principles modeling to investigate the influence of Th and grain boundary on mechanical properties and stability of UO_2 nuclear fuels. By calculating incorporation energy of He and mechanical properties we concluded that Th does not affect the stability of SNFs significantly. Among the various grain boundaries, we chose Σ3 (111)/[110] tilt grain boundary to see stability of He. We found that this grain boundary is a more thermodynamically stable position for He than bulk grain.

Acknowledgment

The Nuclear R&D Program funded by the Ministry of Science and ICT (2016M2B2B1945254) supported this research. This work was also supported by the Global Frontier Pro-gram through the Global Frontier Hybrid Interface Materials (GFHIM) (2013M3A6B1078882) funded by the Mistry of Science and ICT.

References

1. Högselius, P., "Spent Nuclear Fuel Policies in Historical Perspective: An International Comparison," *Energ. Policy*, **37**(1), 254-263(2009).
2. Bunn, M., Holdren, J. P., Fetter, S. and van Der Zwaan, B., "The Economics of Reprocessing Versus Direct Disposal of Spent Nuclear Fuel," *Nucl. Technol*., **150**(3), 209-230(2005).
3. Ewing, R., Weber, R. W. and Clinard Jr., F., "Radiation Effects in Nuclear Waste Forms for High-level Radioactive Waste," *Prog. Nucl. Energ*., **29**(2), 63-127(1995).
4. Gryaznov, D., Heifets, E. and Kotomin, E., "Ab Initio DFT+U Study of He Atom Incorporation into UO_2 Crystals," *Phys. Chem. Chem. Phys*., **11**(33), 7241-7247(2009).
5. Yun, Y., Eriksson, O. and Oppeneer, P. M., "Theory of He Trapping, Diffusion and Clustering in UO_2," *J. Nucl. Mater*., **385**(3), 510-516(2009).
6. Liu, X.-Y. and Andersson, D., "Molecular Dynamics Study of Fission Gas Bubble Nucleation in UO_2," *J. Nucl. Mater*., **462**, 8-14(2015).
7. Govers, K., Lemehov, S., Hou, M. and Verwerft, M., "Molecular Dynamics Simulation of Helium and Oxygen Diffusion in $UO_{2\pm x}$," *J. Nucl. Mater*., **395**(1-3), 131-139(2009).
8. Dabrowski, Ludwik, and Marcin Szuta. "Diffusion of Helium in the Perfect and Non Perfect Uranium Dioxide Crystals and Their Local Structures," *J. Alloys Compd*., **615**, 598-603(2014).
9. Liu, X.-Y. and Andersson, D., "Revisiting the Diffusion Mechanism of Helium in UO_2: A DFT+ U Study," *J. Nucl. Mater*., **498**, 373-377(2018).
10. Thompson, A. E. and Wolverton, C., "First-principles Study of Noble gas Impurities and Defects in UO_2," *Phys. Rev. B*, **84**(13), 134111(2011).
11. Lederer, C., Hollander, J. and Perlman, S., "Table of Isotopes 6th edn," Wiley, New York, 5-6(1968).
12. Olander, D. R., "Fundamental Aspects of Nuclear Reactor Fuel Elements," California Univ., Berkeley (USA). Dept. of Nuclear Engineering, 1976.
13. Ewing, R. C., "Long-term Storage of Spent Nuclear Fuel," *Nat. Mater*., **14**(3), 252(2015).
14. Nerikar, P. V., Rudman, K., Desai, T. G., Byler, D., Unal, C., McClellan, K. J., Phillpot, S. R., Sinnott, S. B., Peralta, P., Uberuaga, B. P. and Stanek, C. R., "Grain Boundaries in Uranium Dioxide: Scanning Electron Microscopy Experiments and Atomistic Simulations," *J. Am. Ceram. Soc*., **94**(6), 1893-1900(2011).
15. Kresse, G. and Furthmüller, J., "Efficiency of Ab-initio Total Energy Calculations for Metals and Semiconductors Using a Plane-wave Basis Set," *Comput. Mater. Sci*., **6**(1), 15-50(1996).
16. Perdew, J. P., Burke, K. and Ernzerhof, M., "Generalized Gradient Approximation Made Simple," *Phys. Rev. Lett*., **77**(18), 3865(1996).
17. Perdew, J. P. and Burke, K., "Comparison Shopping for a Gradient-corrected Density Functional," *Int. J. Quantum. Chem*., **57**(3), 309-319(1996).
18. Blöchl, P. E., "Projector Augmented-wave Method," *Phys. Rev. B*, **50**(24), 17953(1994).
19. Brincat, N. A., Molinari, M., Parker, S. C., Allen, G. C. and Storr, M. T., "Computer Simulation of Defect Clusters in UO_2 and Their Dependence on Composition," *J. Nucl. Mater*., **456**, 329-333(2015).
20. Dorado, B., Freyss, M., Amadon, B., Bertolus, M., Jomard, G. and Garcia, P., "Advances in First-principles Modelling of Point Defects in UO_2: f electron Correlations and the Issue of Local Energy Minima," *J. Phys. Condens. Matter*., **25**(33), 333201(2013).
21. Meredig, B., Thompson, A., Hansen, H. A., Wolverton, C. and Van de Walle, A., "Method for Locating Low-energy Solutions Within DFT+ U," *Phys. Rev. B*, **82**(19), 195128(2010).
22. Idiri, M., Bihan, T. L., Heathman, S. and Rebizant, J., "Behavior of Actinide Dioxides Under Pressure: UO_2 and ThO_2," *Phys. Rev. B*, **70**(1), 014113(2004).
23. Yun, Y. S., Oppeneer, P. M., Kim, H. and Park, K., "Defect Energetics and Xe Diffusion in UO_2 and ThO_2," *Acta Metall*., **57**(5), 1655-1659(2009).
24. Yun, Y., Eriksson, O. and Oppeneer, P. M., "First-principles Modeling of He-clusters in UO_2," *J. Nucl. Mater*., **385**(1), 72-74(2009).
25. Sanati, M., Albers, R. C., Lookman, T. and Saxena, A., "Elastic Constants, Phonon Density of States, and Thermal Properties of UO_2," *Phys. Rev. B*, **84**(1), 014116(2011).
26. Sisodia, P., Dhoble, A. and Verma, M., "Shear Moduli of Macroisotropic Cubic Polycrystalline Materials," *Phys. Status. Solidi. B*, **163**(2), 345-354(1991).
27. Klein, C. A. and Cardinale, G. F., "Young's Modulus and Poisson's Ratio of CVD Diamond," *Diam. Relat. Mater*., **2**(5-7), 918-923(1993).
28. Munro, R. G., "Elastic Moduli Data for Polycrystalline Oxide Ceramics," NIST. No. NIST Interagency/Internal Report (NISTIR)-6853(2002).
29. Kanchana, V., Vaitheeswaran, G., Svane, A. and Delin, A, "First-principles Study of Elastic Properties of CeO_2, ThO_2 and PoO_2," *J. Phys. Condens. Matter*., **18**(42), 9615(2006).
30. Jang, Bo Gyu, Seung Ill Hyun, Moo Hwan Kim, Massoud Kaviany, and Ji Hoon Shim, "Origin of f-orbital-bonding insensitivity to spin-orbit coupling in UO_2," *EPL*, **112**(1), 17012(2015).
31. Fritz, I., "Elastic Properties of UO_2 at High Pressure," *J. Appl. Phys*., **47**(10), 4353-4358(1976).
32. Macedo, P., Capps, W. and Wachtman Jr. J., "Elastic Constants of Single Crystal ThO_2 at 25 °C," *J. Am. Ceram. Soc*., **47**(12), 651-651(1964).